PERGAMON

International Journal of Heat and Mass Transfer 43 (2000) 53–67

International Journal of
HEAT and MASS
TRANSFER

www.elsevier.com/locate/ijhmt

Conjugate forced convection and heat conduction with freezing of water content in a plate shaped food

Nelson O. Moraga*, Enzo E. Medina

Departamento de Ingeniería Mecánica, Universidad de Santiago de Chile, Casilla 10233, Correo 2, Santiago, Chile

Received 5 February 1998; received in revised form 1 April 1999

Abstract

The finite volume method is used to describe unsteady forced convection and heat conduction in a meat plate during freezing. External fluid mechanics and internal solidification of water content in the meat are predicted from a mathematical model that includes continuity, Navier–Stokes and energy equations for air around the food and the heat diffusion equation inside the meat. Unsteady results are presented for both velocity vectors and temperature distributions in air, temperature variations in the food and for heat transfer coefficients. Experimental data for the temperature variation in time are used to assess the accuracy of the predicted values.

1. Introduction

Life and quality of solid foods such as meats, fish, fruits and vegetables are influenced by bacteria, yeasts, molds, viruses and other microorganisms that are present in living organisms and in the air in contact with them. At the low temperatures used in freezing, the microorganisms can be controlled by inhibiting their rate of growth and hence, the storage life of perishable foods can be extended by months, while the rate of freezing has a major effect on the small size of ice crystals that are desirable to obtain good quality, texture, nutritional and sensory properties of foods [1].

The design of freezing processes and equipment are heavily based on the knowledge available to describe the transient heat conduction with solidification of the water content in the food [2]. In general, the approach used to predict the heat transfer processes during food freezing is based on solving the heat diffusion equation with external boundary conditions of the third kind [3,4]. The non-linear nature of the mathematical model caused by temperature variations of the food thermal conductivity, specific heat, enthalpy and density [5,6] and the phase transformation of the liquid water content into ice, have motivated the use of numerical methods to solve the discretized version of the heat diffusion with a phase change model. Among them, finite differences methods with explicit, implicit, Lees and Crank-Nicolson time integration schemes have been most often used [7–14,49]. Finite elements methods have been implemented to describe heat conduction for irregularly shaped foods [15–19], even though it has been found that greater computer times are required than that for finite difference methods [20,21]. A boundary-fitted grid numerical method has been implemented to predict freezing times of arbitrary shaped foods with similar accuracy than finite elements calculations and shorter computer times [22]. Shape specific predictions methods based on geometric factors, have been developed to predict freezing times for regular and irregular foods as an alternative to numerical

* Corresponding author. Tel.: +56-52-682-5498; fax: +56-52-682-5498.

E-mail address: nmoraga@lauca.usach.cl (N.O. Moraga)

0017-9310/00/$ - see front matter
PII: S0017-9310(99)00119-2

Nomenclature

a	length of the plate shaped food [m]
A	length of the computational domain [m]
b	height of the plate shaped food [m]
B	height of the computational domain [m]
c_p	apparent specific heat of the food [kJ kg^{-1} $°C^{-1}$]
h	local heat transfer coefficient [W m^{-2} K^{-1}]
k	thermal conductivity [W m^{-1} $°C^{-1}$]
n	normal direction to food surface
p	pressure [N m^{-2}]
q	heat flux [W m^{-2}]
Re	Reynolds number, $U_0 a/\nu$
t	time [s]
T	temperature [°C]
T_0	initial air and food temperature [°C]
u	x-direction velocity [m s^{-1}]
U_0	x-direction velocity at $x = 0$ [m s^{-1}]
v	y-direction velocity [m s^{-1}]
w	under-relaxation factor
x	horizontal coordinate [m]
y	vertical coordinate [m].

Greek symbols

α	thermal diffusivity [m^2 s^{-1}]
μ	dynamic viscosity [N s m^{-2}]
ν	kinematic viscosity [m^2 s^{-1}]
ρ	density [kg m^{-3}].

Subscripts

a	air
f	fluid
s	solid
w	outer wall of the food
1	after the food
0	initial.

methods [23,24], however, the variations of the geometric factors with thermal properties, final thermodynamic center temperature, Stefan and Planck numbers are ignored.

The value of heat transfer coefficient h has been acknowledged to be one of the major error sources in numerical and approximate solutions for freezing time predictions [7]. One of the methods often used to obtain h is based on the transient lumped heat capacity heat transfer model by measurements of the temperature variations in time on metals with the same dimensions of the food [25–28]. However, the assumptions used to derive the equation for h requires that the cooling fluid temperature remains constant with time, and the specific heat of the solid be independent of temperature variations, two situations that are not always true in food freezing. The convective heat transfer coefficient has also been determined for spherical foods by specifying numerically h values that give the best agreement with measured temperature profiles [27,29–31]. Some of the shortcomings in commonly used experimental methods for food freezing predictions have been shown to be related to the measurement of the heat transfer coefficient, and in maintaining a uniform h across food samples [32], since the convective heat coefficient can vary with time and with the surface location respect to the external fluid flow [7]. Heat transfer coefficients measured at the surface of elliptical cylinders placed in cross flows of air, in the velocity range 0.5–2 m/s that is characteristic of food pilot plants, have been found to be higher than those values which are measured in aeronautical wind tunnels [33]. Furthermore, in food chilling, using air at moderate speeds and in processes with low h values, it has been found by using a finite element method, that a small deviation in surface heat coefficient may result in large deviations in the core temperature for foods with slab, cylinder and sphere shapes [34].

The purpose of this study is to solve the freezing problem for a plate shaped food, using the finite volume method, without the use of a heat convective coefficient as an external boundary condition that has been found to be a major error source in existing numerical and approximate solutions [7,32–34]. The conjugate study proposed considers that the diffusion equation in the food is a simplified version of the unsteady energy equation for the air in contact with it, in which the food can be assumed as a fluid having an infinitely large viscosity, therefore the flow inside it is suppressed. Thermal properties for the air are switched to the temperature dependent ones for the food in the corresponding subregion where it stands. The phase change of the liquid water to ice in the food is incorporated in the mathematical model by an apparent specific heat [35] that is changing with temperature. The numerical simulation of unsteady forced convection heat transfer includes the heat conduction with the solidification of the water content in the food. The conjugate heat transfer model is described by two coupled energy equations, one for the air and the other for the freezing food that includes the phase change of liquid water to ice, and the unsteady Navier–Stokes equations. The finite volume method, with the SIMPLE algorithm [36], is used to solve the system of discretized governing equations. Experiments for freezing of a plate shaped salmon meat portion inside a chamber in which air is initially at rest at ambient temperature equal to the food, are performed to measure unsteady temperatures in the food with thermocouples and to assess the accuracy of the mathematical model and the numerical solution procedure.

The numerical model used for predicting heat transfer and fluid flow in food freezing has been published recently elsewhere, where the thermodynamic model used to calculate the temperature dependence of the thermal properties has been presented in detail, along with the grid independent tests performed for velocity, pressure and temperature calculations [37]. The present paper presents unique results of the prediction for the transient evolution of the temperature distribution inside the food, that shows a faster cooling of the portion of food facing cool air, and of the variations in time, of the heat transfer coefficients along the four external surfaces of the food, that were calculated after the mathematical model was solved and the temperature distribution in the air was obtained. The conjugate study performed, removes the uncertainty in the use of a heat transfer coefficient in the calculations, that is not always available with the required accuracy, and it can be extended to foods with irregular shapes. A more accurate freezing time information is obtained in food sections near to regions where the fluid dynamics and the convective heat transfer change rapidly in time and space.

2. Physical situation and mathematical model

A plate shaped portion of salmon meat of length a by height b at the initial uniform temperature T_0, is placed in a horizontal position inside a freezing chamber with air at rest, at ambient temperature T_0. A refrigeration unit is put to work and the air starts flowing around the food and the air temperature begins to quickly decrease until a thermostat stops the refrigeration cycle for the first time at around 1270 s, when the air temperature in the chamber is −29°C. Heat transfer from the outside, through the chamber walls, increases the air temperature in the chamber until it reaches −24°C activating the thermostat again, after that, the process is repeated in a cyclical fashion. Fig. 1 shows a schematic view of the physical situation and the system of Cartesian coordinates used in the mathematical model.

In the formulation of the conjugate heat transfer problem, the following assumptions are made: air is a Newtonian, incompressible fluid with constant properties, the flow is unsteady and two-dimensional; the food is a binary mixture of solid and water that can be either in liquid phase or partially in solid phase, as ice, with temperature dependent: density, specific heat and thermal conductivity. Under this assumption the governing mass conservation, Navier–Stokes and energy equations for the air flow are:

$$\frac{\partial u}{\partial x} + \frac{\partial v}{\partial y} = 0 \tag{1}$$

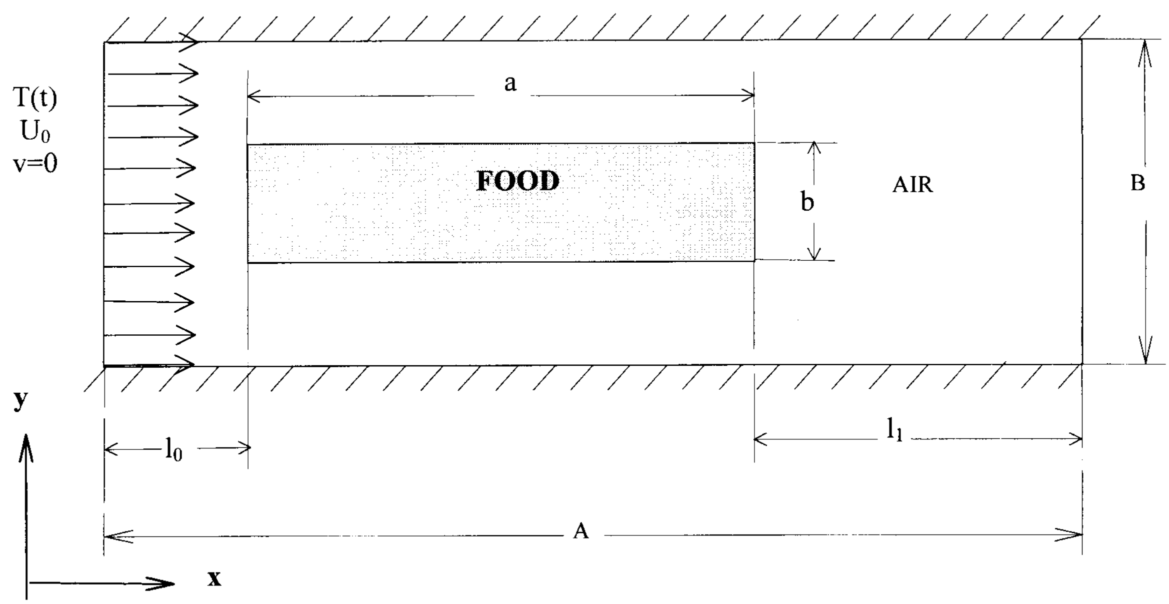

Fig. 1. Physical situation.

$$\rho_a\left(\frac{\partial u}{\partial t}+u\frac{\partial u}{\partial x}+v\frac{\partial u}{\partial y}\right)=\mu_a\left(\frac{\partial^2 u}{\partial x^2}+\frac{\partial^2 u}{\partial y^2}\right)-\frac{\partial p}{\partial x} \quad (2)$$

$$\rho_a\left(\frac{\partial v}{\partial t}+u\frac{\partial v}{\partial x}+v\frac{\partial v}{\partial y}\right)=\mu_a\left(\frac{\partial^2 v}{\partial x^2}+\frac{\partial^2 v}{\partial y^2}\right)-\frac{\partial p}{\partial y} \quad (3)$$

$$\frac{\partial T}{\partial t}+u\frac{\partial T}{\partial x}+v\frac{\partial T}{\partial y}=\alpha_a\left(\frac{\partial^2 T}{\partial x^2}+\frac{\partial^2 T}{\partial y^2}\right) \quad (4)$$

and the heat diffusion equation for the salmon meat is:

$$\frac{\partial}{\partial t}(\rho c_p T)=\frac{\partial}{\partial x}\left(k\frac{\partial T}{\partial x}\right)+\frac{\partial}{\partial y}\left(k\frac{\partial T}{\partial y}\right) \quad (5)$$

The properties of the air are assumed to be constant during the process: $\mu=1.8224\times10^{-5}$ kg/(m s); $\rho=1.3$ kg/m^3; k = 0.0251 W/(m °C); $c_p=1.01$ kJ/(kg °C). A thermodynamic model that considers food as an ideal binary solution of pure water and solids is used to calculate the temperature variations for the properties of salmon meat. The predicted method required the following input values under unfrozen conditions: initial freezing temperature = −2.2°C; initial moisture content = 64%; $c_p=3.153$ kJ/(kg °C); k = 0.481 W/m °C; $\rho=1100$ kg/m^3; unfreezable water content = 9%. A temperature dependent apparent specific heat, calculated from the values of specific heat of the food considering water in liquid and solid phases in addition to the latent heat, as an extension of the definition found in the literature [35], was used during the phase change of water. The complete model has been presented elsewhere [37] together with the values of the five coefficients used to approximate by least square fitting, the values calculated of the density, specific heat and thermal conductivity in terms of fifth degree polynomial functions of temperature, for the temperature range: $-29°C \le T < 25°C$, divided in five temperature ranges.

The initial conditions at time t equals 0 are:

$$u=v=0;\quad T_{air}=T_{food}=T_0=17.8°C \quad \text{at } t=0 \quad (6)$$

the boundary conditions for the conjugate problem are:

$$u=U_0=3.3\text{ m/s};\quad v=0;$$
$$T=a-b\ \ln(t)+c\ \sin(dt) \quad \text{at } x=0 \quad (7)$$

$$\frac{\partial u}{\partial x}=\frac{\partial T}{\partial x}=v=0 \quad \text{at } x=A \quad (8)$$

$$\frac{\partial u}{\partial y}=\frac{\partial T}{\partial y}=v=0 \quad \text{at } y=0 \quad (9)$$

$$\frac{\partial u}{\partial y}=\frac{\partial T}{\partial y}=v=0 \quad \text{at } y=B \quad (10)$$

where the constants a, b, c and d used in the mathematical description of the time variation of air temperature are found from experimental data, as indicated in the experimental procedure section.

3. Numerical solution procedure

The nonlinear, unsteady mathematical model for coupled forced convection to heat conduction with

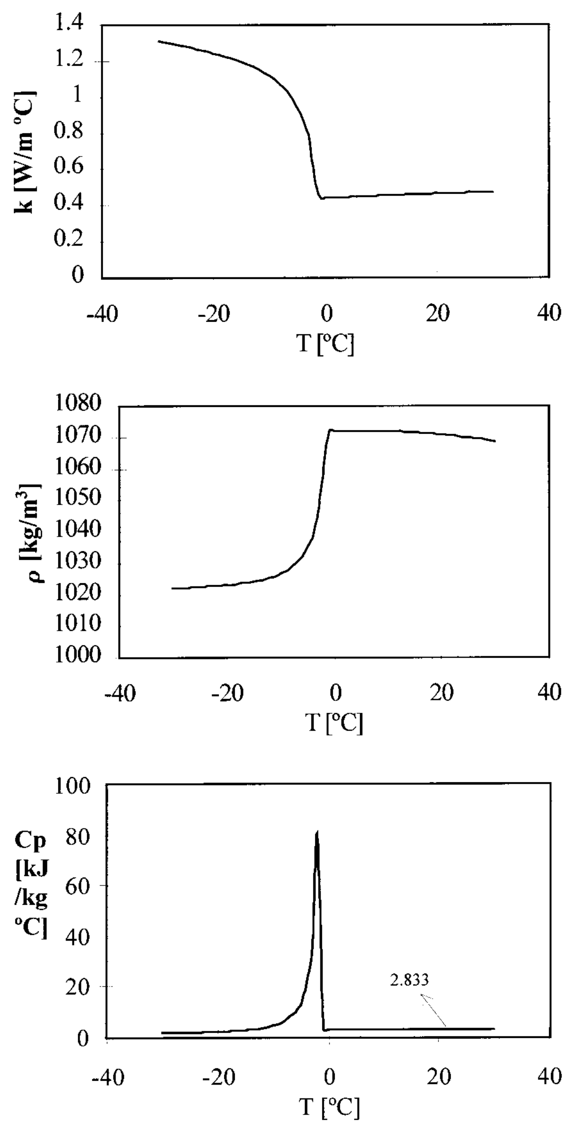

Fig. 2. Temperature dependence of salmon meat properties.

liquid–solid phase transformation of the water content in the food was solved by the finite volume method [36].

A staggered grid was used to calculate pressure and temperature at the grid points located in the center of the finite volumes obtained after the discretization of the domain and the velocity components in the cell faces between the nodes [36].

The calculation of pressure and velocities for air flow around the food was done iteratively using the Semi-Implicit Method for Pressure-Linked Equations, SIMPLE algorithm [36]. The discretized momentum equations were solved to obtain the velocity components (u^*, v^*) with an initial guessed pressure field (p^*). Then the values of the calculated velocities were replaced in the discretized continuity equation to get a pressure correction (p') that allowed us to obtain correction values for the velocities (u', v'). Corrected values for p, u, v were calculated using under-relaxation during the iterative process [42].

$$p^{\text{new}} = p^* + w_{\text{p}} p'; \quad u^{\text{new}} = w_{\text{u}} u + (1 - w_{\text{u}}) u^{k-1}; \quad v^{\text{new}} = w_{\text{v}} v + (1 - w_{\text{v}}) v^{k-1} \tag{11}$$

where the under-relaxation factors used were $w_{\text{u}} = w_{\text{v}} = 0.5$ and $w_{\text{p}} = 0.8$.

The next step was to solve the discretized energy equation to obtain the temperature field. Calculations in the food were performed by imposing in this subdomain, a large value of the kinematic viscosity $\nu = 10^{20}$ m^2/s and switching from the air properties to the temperature dependent salmon meat properties that are shown in Fig. 2. The iterative procedure was stopped when the discretized continuity equation was satisfied in all cells and the mass source [36] generated in each control volume was lower than 10^{-6}.

Piecewise linear interpolation profiles were used for temperature and the velocity components in the calculation of the diffusion terms of the governing equations and convective terms were calculated by the power-law scheme described by Patankar [36]. A line by line numerical method was used to solve the discretized system of equations [36].

Boundary conditions between the solid (meat) and the fluid (air) were [39]

$$(T_{\text{s}})_{\text{w}} = (T_{\text{f}})_{\text{w}}; \quad -k_{\text{s}} \left(\frac{\partial T_{\text{s}}}{\partial n} \right)_{\text{w}} = -k_{\text{f}} \left(\frac{\partial T_{\text{f}}}{\partial n} \right)_{\text{f}} \tag{12}$$

The temperature gradients in the solid and in the fluid were calculated in the normal direction to the wall in the following way

$$\left(\frac{\partial T_{\text{s}}}{\partial n} \right)_{\text{w}} = \frac{T_{\text{s}} - T_{\text{w}}}{\Delta n_{\text{s}}}; \quad \left(\frac{\partial T_{\text{f}}}{\partial n} \right)_{\text{w}} = k_{\text{f}} \frac{T_{\text{w}} - T_{\text{f}}}{\Delta n_{\text{f}}} \tag{13}$$

The calculation domain was discretized in such a fashion that the faces of the control volumes used to calculate temperature coincide with the faces of the control volumes and hence, on the meat walls no node was located. Therefore, in the last equation T_{s} and T_{f} were the temperatures of two neighbor-points in the same spatial direction, for the last node in the food and for the first node in the fluid around the food in the normal direction to the external surface of the meat, located at distances $\Delta n_{\text{s}} = \Delta n_{\text{f}}$, equals to the half separation between nodes, from the interface between meat and air. The unknown temperature in the meat wall T_{w} was obtained from an energy balance,

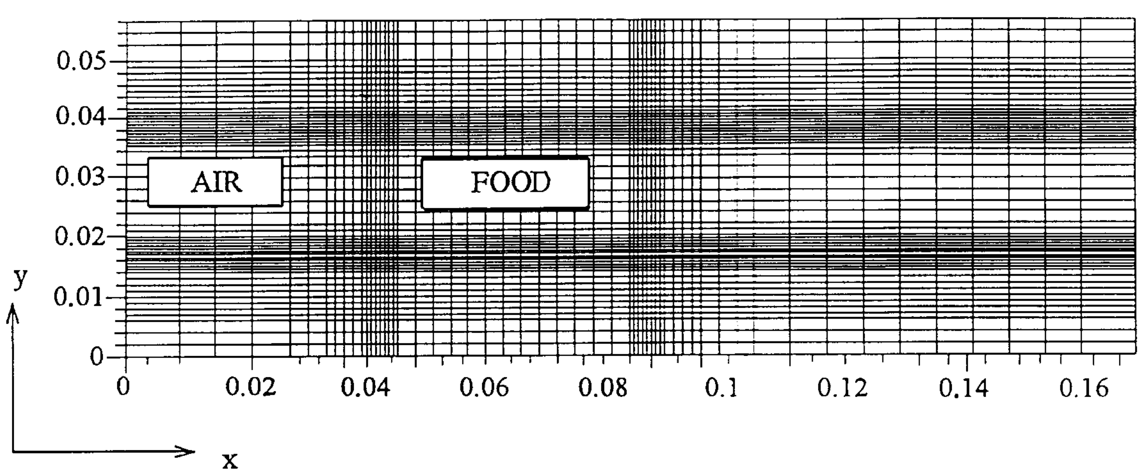

Fig. 3. Discretized domain.

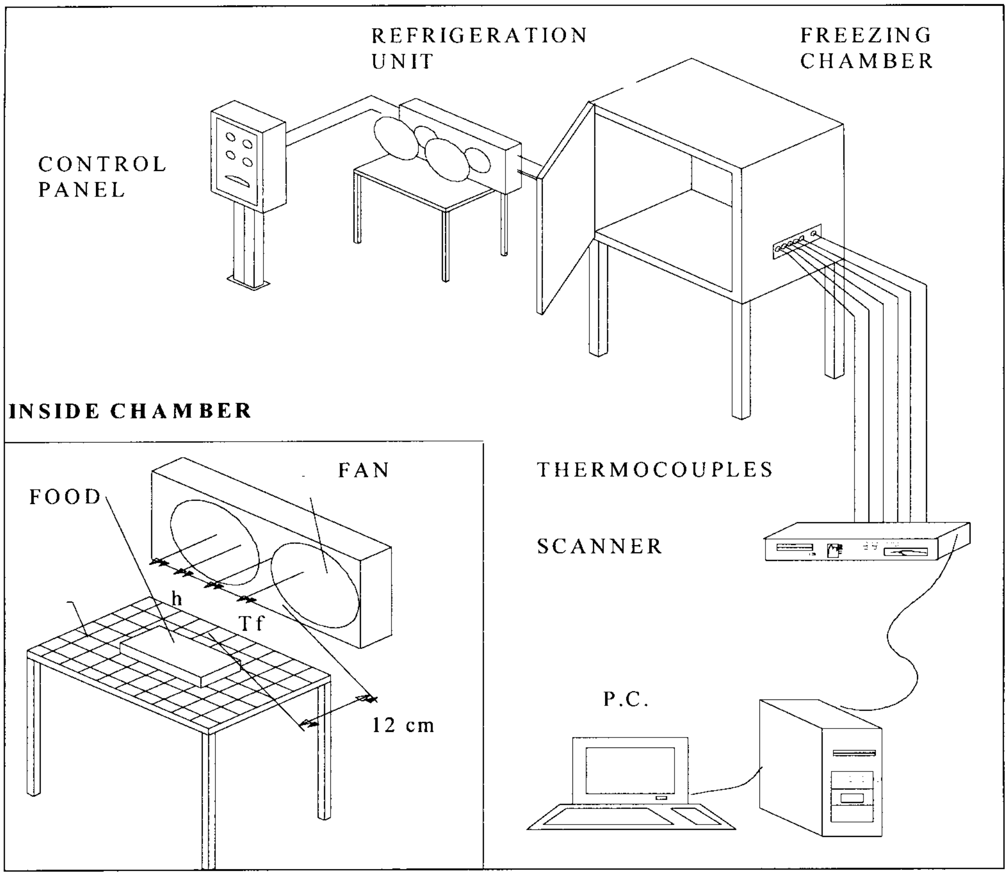

Fig. 4. Schematic view of experimental facility.

$$T_w = \frac{K_s T_s + K_f T_f}{K_s + K_f}; \quad K_s = \frac{k_s}{\Delta n_s}; \quad K_f = \frac{k_f}{\Delta n_f} \tag{14}$$

After several trials with different grids, the nonuniform grid shown in Fig. 3 with 59 nodes in each spatial direction was found to be efficient for the numerical calculations. Time steps of 0.001 s were used during the first 5 s to solve the forced convection-phase change heat conduction problem. After 5 s the fluid mechanics yield to a steady state and hence that calculation for the Navier–Stokes and continuity equations stopped and the energy equation for air coupled to the heat diffusion equation was solved from that instant on with time steps equal to 0.1 s. Nodes located at selected spatial locations were used to control convergence for predicted pressure, velocity and temperature in the air, while numerical results for temperature in the food were compared with experimental data at the locations of the thermocouples, for time steps of 0.1, 0.01 and 0.001 s that were used to describe the

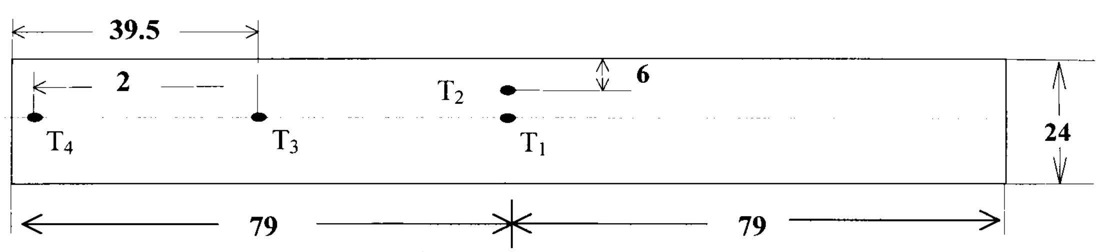

Fig. 5. Thermocouple locations inside the food.

unsteady fluid mechanics around the food. Results of time and grid independent tests performed with a different solution algorithm, SIMPLER, for the same problem, have been given elsewhere [37]. The time steps used with the SIMPLE algorithm: $\Delta t = 0.001$ for $t \leq 5$ s and $\Delta t = 0.1$ for $t > 5$ s were smaller than those values $\Delta t = 0.0025$ s and $\Delta t = 0.5$ s used along with the calculations performed with the SIMPLER algorithm [37].

4. Experimental procedure

A salmon meat freezing experiment was conducted to measure the time history of temperature in the food at four locations and the surrounding air temperature. The experimental facility shown in Fig. 4 included a cooling chamber of internal volume equal to 0.6 m^3, a refrigeration unit with two fans. *T*-type thermocouples, 0.3 mm in diameter and 1.5 in length, with a $\pm 1\%$ accuracy were connected to a Cole Parmer Scanner and to a personal computer, where temperatures were recorded at 2 s intervals by using a MAC-14 computer program.

A portion of salmon meat with a water content of 64% was shaped into a plate geometry of 24 mm in height and 158 mm in length. The plate shaped food was put on a net built with thread of 0.1 mm in diameter. Four thermocouples were inserted in the food in the spatial locations shown in Fig. 5. Air temperature at the location l_o before the food, as shown in Fig. 1, was measured at 2 s time intervals to capture its unsteady variation from the initial ambient temperature $T_0 = 22$°C. Air temperature changed rapidly with time initially in a monotonous decreasing fashion after the refrigeration unit was put to work, and later in an oscillating way due to the action of a thermostat that shut down and put to work at time intervals in the refrigeration process when a temperature of -25°C was reached in the chamber. The unsteady air temperature

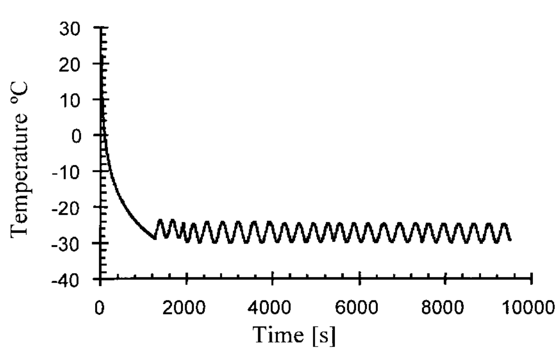

Fig. 6. Unsteady air temperature inside the freezing chamber.

Table 1
Value of constants to describe the unsteady air temperature in Eq. (7)

$a = 15.0$; $b = 0$; $c = 0$ for $t \leq 10$ s
$a = 49.201$; $b = 11.0708$; $c = 0$ for $10 < t \leq 1270$ s
$a = 27.4210$; $b = 2.6181$; $c = 0.01901$ for $1270 < t \leq 8000$ s

measured at time intervals of 2 s in the chamber, shown in Fig. 6, allowed us to find by the least squares fitting procedure the following values for the constant *a, b, c* and *d* of the equation [7] used in the mathematical model (Table 1).

5. Results and discussion

In this section the distributions of the air velocity around the plate shaped food and of the temperature field inside the food are shown during the unsteady period. Also, a comparison between experimental data for the transient response of the temperature at four different locations and the predicted values obtained from the numerical simulation is made. In addition, local convective heat transfer coefficients on the four surfaces of the food plate are calculated and the results presented.

The accuracy of the finite volume method was estimated first by solving a transient fluid mechanics problem in which isothermal air flows around a square plate with a Reynolds number equal to 10,000. Fig. 7 shows that the results of the stream function in the vicinity of the plate for a time equal to 2 s. The location of the separation points and the extension of vertical and longitudinal recirculation regions agree within 5% with the results obtained by Roland et al. [38] by making use of the random vortex method.

Fig. 8 shows the time evolution of the velocity vectors for air around the plate shaped food with a Reynolds number equal to 6000, at four time intervals in the range between 0.25 s and 2 s. The unsteady calculations were performed with a time step of 0.0001 s and it was found that velocity and pressure distributions did not change after 2 s. Therefore, it was concluded that in that time the fluid mechanics reaches a quasi steady state and the numerical procedure could be simplified by solving only the unsteady energy equation in the fluid with the local values of the velocity components corresponding to the time instant of 2 s. Time steps were incremented to 0.1 s from then on, since the discretized continuity and linear momentum equation no longer needed to be solved and with this time step temperatures in the nodes located in the fluid and inside the food had the required convergence.

Fig. 9 shows the spatial temperature distribution

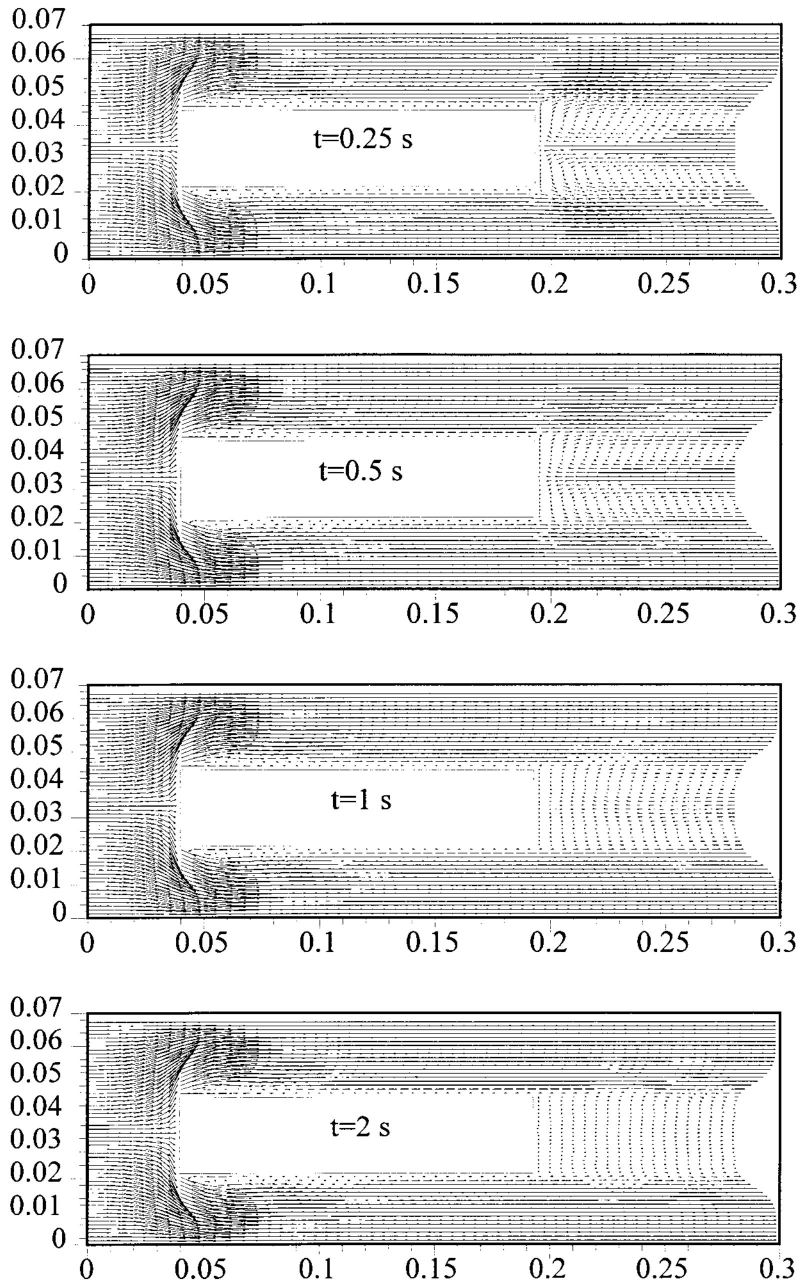

Fig. 7. Stream function for air flow around a square plate, Re = 10,000; t = 2 s.

inside the plate shaped portion of salmon meat, at time intervals of 1000; 2000; 5000; and 8000 s. It can be seen that the temperature field is not symmetric in the streamwise direction and a displacement in the flow direction of the region where temperature is higher occurs during all the cooling process. It can also be observed that the temperature field tends to be uniform for the times between 2000 and 5000 s, when the water content is changing to ice, than at both earlier and later times. This non-symmetric freezing may affect the quality of the food at the regions with higher temperatures, eventually causing fish muscle toughness [40], textural changes [41], modifications of protein in muscle tissue [42,43], denaturation and solubility loss [44] and changes in color and flavor [45].

The temperatures predicted at positions T_3 and T_4,

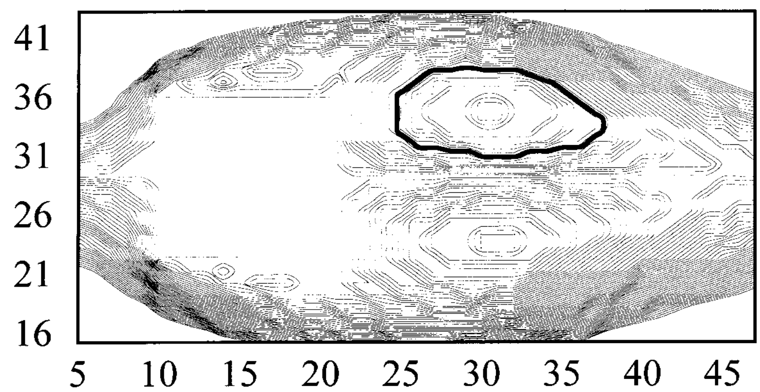

Fig. 8. Velocity vectors around the food at four time instants, Re = 6000.

located closer to the surface facing the air stream, showed better agreement with measured values than the temperature history curves predicted for the geometrical center of the plate, position T_1, and for the position T_2. The maximal temperature differences (equal to 7°C), between predicted and experimental temperature occurs for T_1 in the pre-cooling period, after about 800 s. Mihori and Watanabe [46] have also found with a one-dimensional heat conduction model that worse predictions occurred towards the center of a slab of Alaska Pollark Surimi. The errors in the slower predicted freezing curves could be caused by the values for the food properties used in the numerical model, where according to Hung and Thompson [25], higher values for thermal conductivity and lower values for the specific heat, initial freezing point and amount of unfreezable water would reduce the difference between predicted and measured temperature histories.

A comparison between experimental and predicted freezing times for the four positions where temperature histories were measured in the plate shaped food is presented in Table 2. All data are expressed as percentage differences from experimental data. The comparison is made at two temperature levels: −10°C, that has been used by Cleland and Earle [7], and at −18°C that was the value used to fit data by Hung and Thompson [25].

Table 2
Errors in freezing time predicted by conjugate method at four locations in the food plate

Reference temperature, °C	Error in predicted freezing time, %			
	T_1	T_2	T_3	T_4
−10	1.9	2.9	−8.9	10.6
−18	9.5	10.0	−2.8	5.2

Four semi-empirical freezing time predictions and four based on finite difference methods presented by Cleland and Earle [47], Pham [8], Hung and Thompson [25] and de Michelis and Calvelo [48] were compared with 207 experimental results to −10°C and with 68 experiments to −18°C in [7]. At the higher food center temperature of −10°C the percentage differences for the semi-empirical predictions were between 5.4% [8] and 13.9% [48], while at the lower temperature of −18°C the differences were in the range between 6% [25] and 14.9% [48]. The percentage differences for the finite differences freezing time predictions were found to be within 4.3% [8] and 12.1% [48] at −10°C and between 4.3% [8] and 9.3% [25] at −18°C. In all these comparisons, temperature was measured and calculated at the center of the food under constant ambient temperature. The results presented in Table 2 are calculated and measured at four locations that are different from the thermal center of the plate, while air temperature was changing with time. Even though these two conditions make calculations more complicated, since at the thermal center of the food temperature gradients are equal to zero, the freezing time predictions obtained by the conjugate method are more precise than the ones presented in the references discussed in this section.

In Fig. 10, a comparison is made of the temperature–time evolution at four positions inside the food obtained with the finite volume method and the measured data. It can be observed that the cooling curves at the four locations can be predicted in a reasonable fashion, with difference that are smaller than 6 K. In three locations, the center of the plate, the mid-upper section and in the region closest to the incoming flow direction, the differences between the predicted and measured temperatures are higher for the time before the solid–liquid phase transformation of water.

The local heat transfer coefficients were calculated

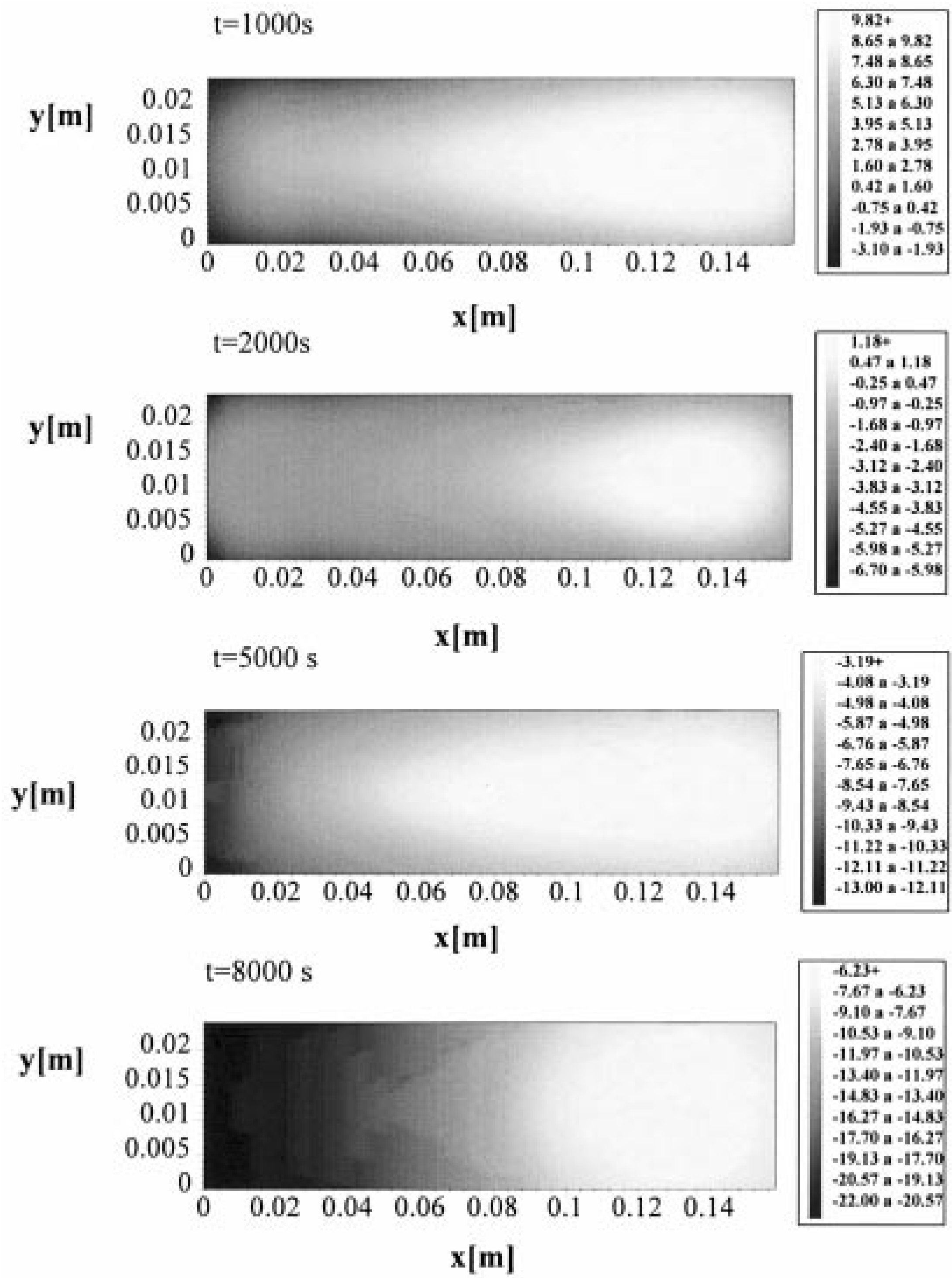

Fig. 9. Temperature distribution inside the food at four time instants.

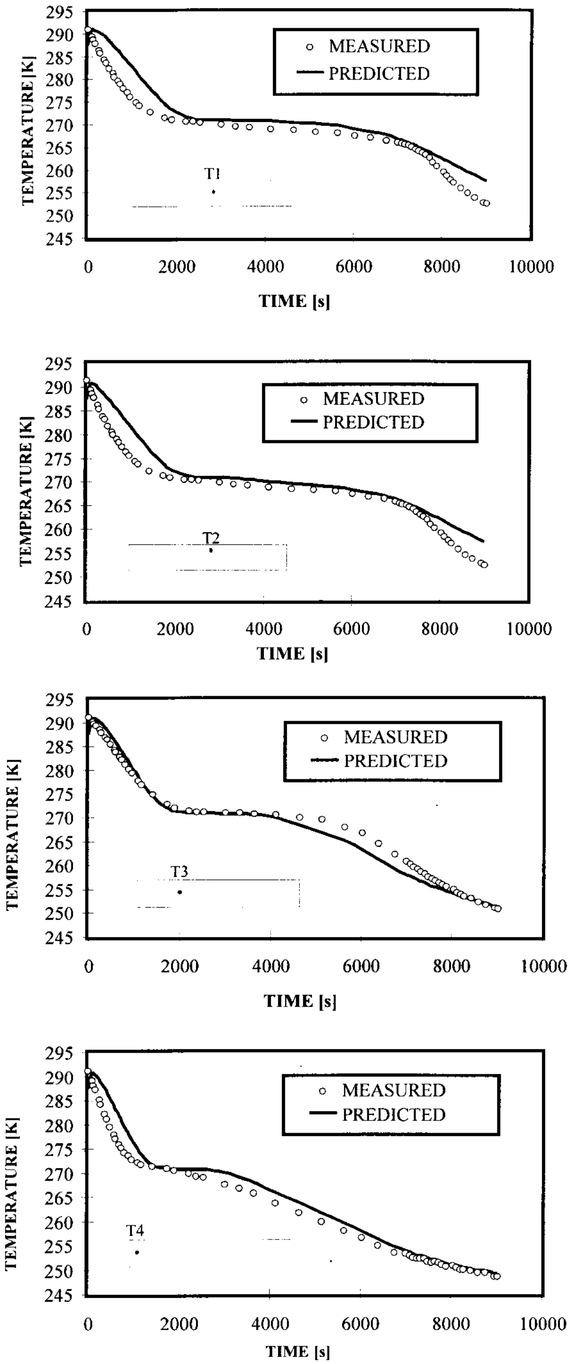

Fig. 10. Cooling curves at four locations inside the food.

after the temperature fields in the food and in the air were computed at each time step from the definition

$$h = \frac{q''}{T_w - T_f}; \quad q'' = \frac{k_s(T_s - T_w)}{\Delta n_s} \tag{15}$$

where the heat flux was found from the heat conduction coming to the outer surface from the neighboring nodes in the food. Figs. 10–14 show the unsteady local heat transfer coefficients at the top, bottom, left and right external surfaces of the food. A sharp drop of the local value of h that decreases to more than half its value is noticed (Figs. 11 and 12) in the first 0.3 cm, facing the cool air incident flow, on top and bottom surfaces. The major changes in the convective heat transfer coefficient can be explained from the results obtained for the predicted velocity and temperature distributions in the air close to the plate walls and from the temperature gradients calculated in the walls of the food. The air stream impinges against the leading vertical wall of the food plate, changes direction and the velocity increases towards the leading corners, where air at a lower temperature comes closer. The lower temperature air flow at high velocity, that originates at the larger value of h at the leading corners, separates from the wall at the two leading corners of the plate and a recirculation zone forms in that first region near the top and bottom surfaces, as is depicted in Fig. 8. The air flowing at low velocity in reverse direction is warmer as a result of the temperature distribution in the food shown in Fig. 9, and hence the lower values of h calculated on those regions. The overall order of magnitude for the heat transfer coefficient in the two horizontal surfaces is similar, $\bar{h} \sim 30$ W/m^2 °C, and the same holds true for the two vertical surfaces that have mean heat transfer coefficients, $\bar{h} =$ 17 W/m^2 °C, being almost two times smaller than the value for the top and bottom surfaces.

A close inspection of Figs. 11 and 12 reveals that the heat transfer coefficient on the top surface is different from the one on the bottom surface, and the same can be observed in the comparison of h values on the upper half with those of the lower half of the vertical walls in Figs. 13 and 14. The fluid mechanics results of the air flow around the plate shows that the forced convection is not completely symmetric in y-direction at the Reynolds number equal to 6000, even though top and bottom surfaces are symmetric with respect to the air flow. The lack of symmetry for the u and v components of the velocity affects the temperature field for the air around the food, causing non symmetric values of h that have differences of about 15%. Results for this lack of symmetry has been presented for isothermal air flow around a square plate at Re = 10,000 [38].

6. Conclusions

A five partial differential equation mathematical model that includes continuity, Navier–Stokes and energy equations for the fluid flow and the heat diffu-

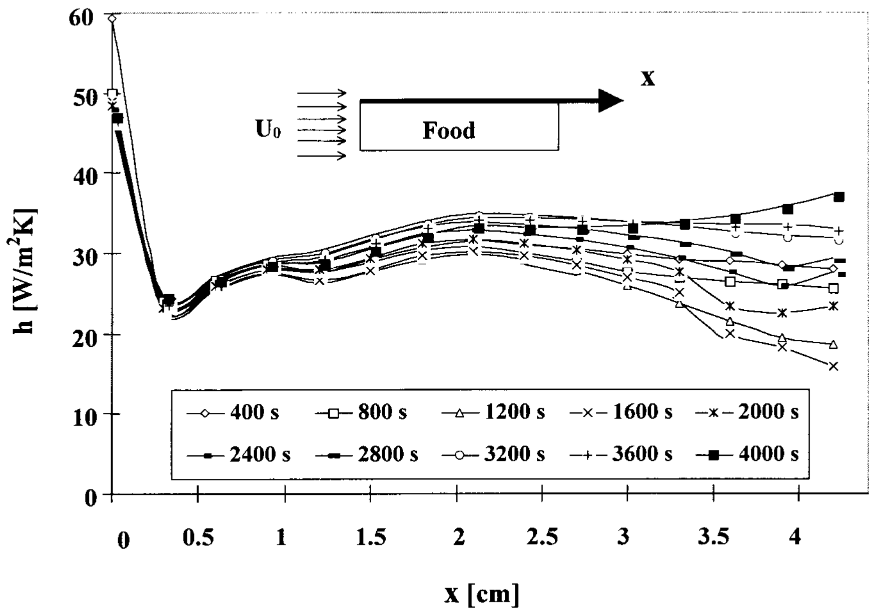

Fig. 11. Unsteady local heat transfer coefficient over top surface of food.

sion equation, with an apparent specific heat have been used to describe the unsteady laminar forced convection coupled to the water solidification problem for freezing plate shaped foods in air initially at rest.

The finite volume method with 58×58 nodes; time steps equal to 0.001 s, for the first 5 s needed to reach the fluid mechanics steady state, and time steps equal to 0.1 s from that instant to the time needed to freeze

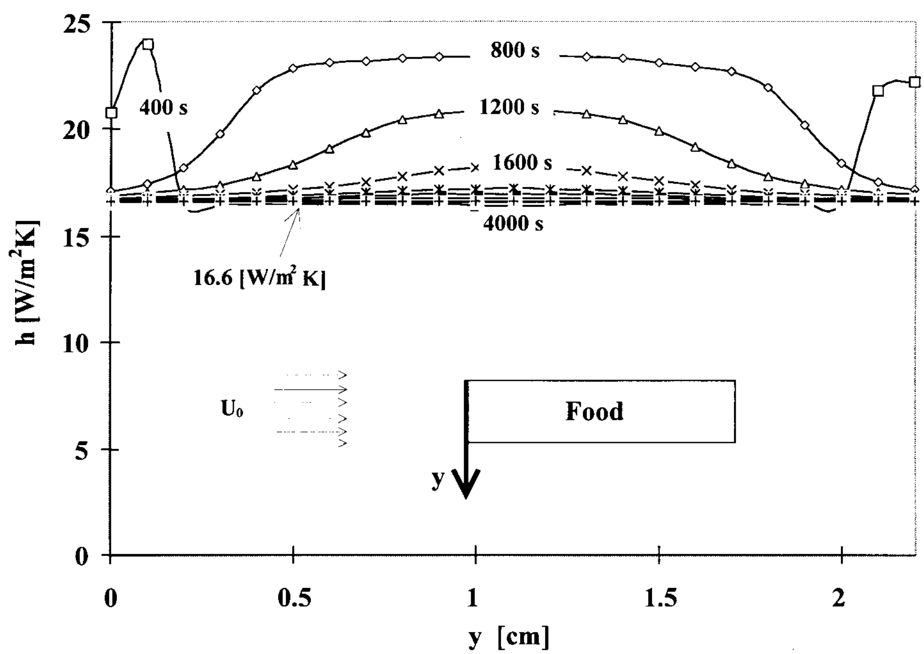

Fig. 12. Unsteady local heat transfer coefficient on bottom surface of food.

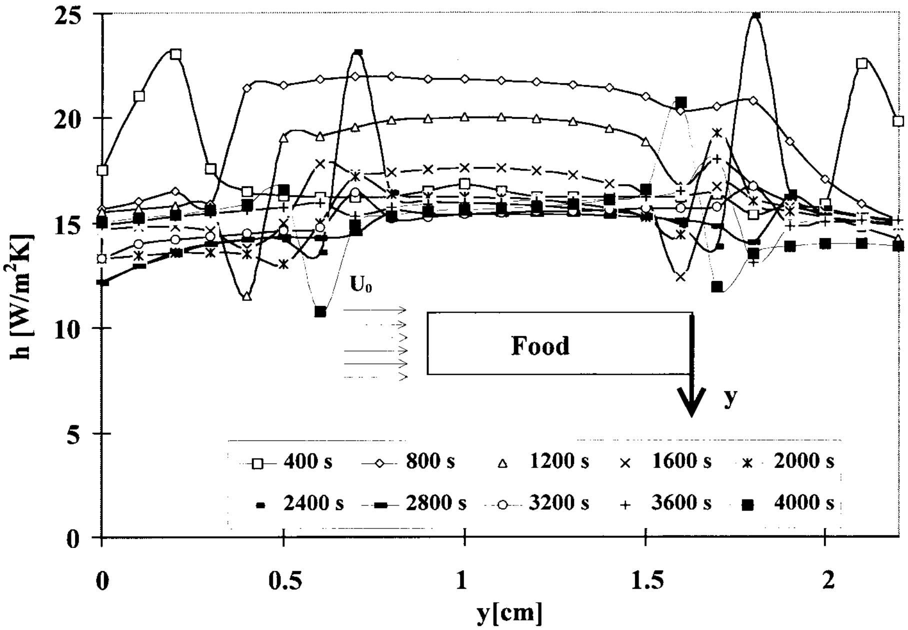

Fig. 13. Unsteady local heat transfer coefficient over surface of food facing the incident air stream.

a portion of salmon meat allowed the prediction of cooling curves. Experimental data for the time variation of the temperature at four locations inside the food was used to validate the numerical prediction. Errors in freezing time predictions at four locations in the food plate by the conjugate method, for time varying cooling air temperature, were in the range between 1.9 and 10.6% at temperatures of −10 and −18°C.

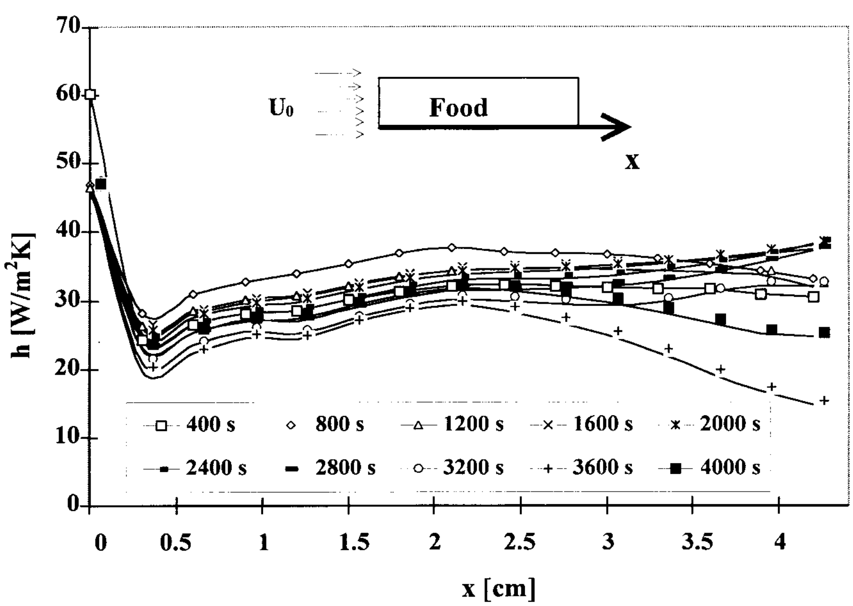

Fig. 14. Unsteady local heat transfer coefficient over surface of food in downstream flow direction.

Acknowledgement

The authors would like to thank Universidad de Santiago de Chile for the support provided to DICYT No. 019916MB project.

References

[1] Y.A. Çengel, Heat Transfer. A Practical Approach, McGraw-Hill, Boston, 1998.
[2] A. Cleland, Food Refrigeration Process. Analysis, Design and Simulation, Elsevier, London, 1990.
[3] A.C. Cleland, R.L. Earle, The third kind of boundary condition in numerical freezing calculations, International Journal of Heat and Mass Transfer 20 (1977) 1029–1034.
[4] S. Thorne, Mathematical Modeling of Food Processing Operations, Elsevier, Essex, 1992.
[5] M.A. Rao, S.S.H. Rizvi, Engineering Properties of Foods, Marcel Dekker, New York, 1995.
[6] R.C. Hsieh, L.E. Lerew, D.R. Heldman, Prediction of freezing times for foods as influenced by product properties, Journal Food Process Engineering 1 (1977) 183–197.
[7] A. Cleland, R. Earle, Assessment of freezing time prediction methods, Journal of Food Science 49 (1984) 1034–1042.
[8] Q. Pham, Note of some finite-difference methods for heat conduction with phase change, Numerical Heat Transfer 11 (1987) 353–359.
[9] H. Wilson, R. Singh, Numerical simulation of individual quick freezing of spherical particles, International Journal of Refrigeration 10 (1987) 149–155.
[10] S. Sheen, K.I. Hayakawa, Finite difference simulation for heat conduction with phase change in an irregular food domain with volumetric change, International Journal of Heat and Mass Transfer 34 (1991) 1337–1346.
[11] B.A. Welt, A.A. Teixeira, K.V. Chau, M.O. Balaban, D.E. Hintenlang, Explicit finite difference methods for heat transfer simulation and thermal process design, Journal of Food Science 62 (1997) 230–236.
[12] Z. Saad, E.P. Scott, Analysis of accuracy in the numerical simulation of the freezing process in food materials, Journal of Food Engineering 31 (1997) 95–111.
[13] C. Ilicali, C. Cettin, S. Cettin, Methods for the freezing time of ellipses, Journal of Food Engineering 28 (1996) 361–372.
[14] A.C. Rubiolo, Average and center time temperature vs time calculation for freezing and thawing rectangular foods, Journal of Food Engineering 30 (1996) 299–311.
[15] G. Comini, S. Del Guidice, R.W. Lewis, O.C. Zienkiewicz, Finite element solution of nonlinear heat conduction problems with special reference to phase change, International Journal Numerical Methods in Engineering 8 (1974) 613–624.
[16] H. Abdalla, R. Singh, Simulation of thawing of foods using finite element method, Journal of Food Process Engineering 7 (1985) 273–286.
[17] V.M. Puri, R.C. Anantheswaran, The finite element method in food processing: a review, Journal of Food Engineering 19 (1993) 242–274.
[18] Wang De Dian, E. Kolbe, Analysis of food block freezing using a PC-based finite element package, Journal of Food Engineering 21 (1994) 521–530.
[19] N. Caroll, R. Mohtar, L.J. Segerlind, Predicting the cooling time for irregular shaped food products, Journal of Food Process Engineering 19 (1986) 385–402.
[20] N. Shamsundar, E. Rooz, Numerical methods for moving boundary problems, in: W.J. Minkowycz, E.M. Sparrow, G.E. Schneider, R.H. Pletcher (Eds.), Handbook of Numerical Heat Transfer, Hemisphere, New York, 1989, pp. 665–676.
[21] D.J. Cleland, A.C. Cleland, R.L. Earle, S.J. Byrne, Prediction of freezing and thawing times for multidimensional shapes by numerical methods, International Journal of Refrigeration 10 (1987) 32–39.
[22] A.N. Califano, N.E. Zaritzky, Simulation of freezing or thawing heat conduction in irregular 2D domains by a boundary-fitted grid method, Lebensmittel-Wissenschaft und-Technologie 30 (1997) 70–76.
[23] D.J. Cleland, A.C. Cleland, R.L. Earle, Prediction of freezing and thawing times for multi-dimensional shapes by simple formulae. Part 2: irregular shapes, International Journal of Refrigeration 10 (1987) 234–240.
[24] V.O. Salvadori, A. Michelis, R.H. Masheroni, Prediction of freezing times for regular multi-dimensional foods using simple formulae, Lebensmittel-Wissenschaft und-Technologie 30 (1997) 30–35.
[25] Y.C. Hung, D.R. Thompson, Freezing time prediction for slab shape foods stuffs by an improved analytical method, Journal of Food Science 48 (1983) 555–560.
[26] K. Suzuki, R.P. Singh, A computer aided calculation of temperature history during thawing of foods, Transactions ASAE 28 (1985) 1330.
[27] C. Ilicali, A simplified analytical model for thawing time calculations in foods, Journal of Food Science 54 (1989) 1031–1036.
[28] H.A. Wilson, R.P. Singh, Numerical simulation of individual quick freezing of spherical foods, Rev. Int. Froid 10 (1987) 149–155.
[29] V.M. Chavarria, D.R. Heldman, Measurement of convective heat transfer coefficients during food freezing processes, Journal of Food Science 49 (1984) 810.
[30] J. Succar, K. Hayakawa, Parametric analysis for predicting freezing time of infinitely slab-shaped foods, Journal of Food Science 49 (1984) 468–477.
[31] C. Bonacina, G. Comini, A. Fasano, M. Primicerio, Numerical solution of phase change problems, International Journal of Heat and Mass Transfer 20 (1973) 1825–1832.
[32] D.J. Cleland, A.C. Cleland, R.S. Jones, Collection of accurate experimental data for testing the performance of simple methods for food freezing time prediction, Journal of Food Process Engineering 17 (1994) 93–119.
[33] A. Kondjoyan, J.D. Daudin, J.J. Bimbenet, Heat and mass transfer coefficients at the surface of elliptical cylinders placed in a turbulent air flow, Journal of Food Engineering 20 (1993) 339–367.

[34] B.M. Nicolai, J. De Baerdemaker, Sensitivity analysis with respect to the surface heat transfer coefficient as applied to thermal process calculations, Journal of Food Engineering 28 (1996) 23–33.
[35] J. Hsiao, An efficient algorithm for finite-difference analyses of heat transfer with melting and solidification, Numerical Heat Transfer 8 (1985) 653–666.
[36] S.V. Patankar, Numerical Heat Transfer and Fluid Flow, Hemisphere, New York, 1980.
[37] N.O. Moraga, C.H. Salinas, Numerical model for heat and fluid flow in food freezing, Numerical Heat Transfer, Part A 35 (1999) 495–513.
[38] W. Roland, H. Sphaier, M. Vaidhyanathan, Unsteady flow about bluff cylinders, International Journal of Offshore and Polar Engineering 3 (1993).
[39] A. Luikov, in: Heat and Mass Transfer, Mir, Moscow, 1980, p. 340.
[40] R.H. Love, Texture and fragility of fish muscle cells, Journal of Texture Stud 14 (1983) 323.
[41] Y.L. Hsieh, J.M. Regenstein, Texture change of frozen stored cod and ocean perch minces, Journal of Food Science 54 (1989) 824–826.
[42] J.F. Ang, H.O. Hultin, Denaturation of cod myosin during freezing after modification with formaldehyde, Journal of Food Science 54 (1989) 814–818.
[43] E.L. LeBlanc, R.J. LeBlanc, Separation of cod (gadus morhua) fillet proteins by electrophoresis and HPLC after various frozen storage treatments, Journal of Food Science 54 (1989) 827–834.
[44] S.Y. Shenouda, Theories of protein denaturation during frozen storage of fish flesh, in: C.O. Chichester, E.M. Mrak, G.F. Stewart (Eds.), Advances in Food Research, vol. 26, Academic Press, New York, 1980, p. 275.
[45] M.C.M. Banda, H.O. Hultin, Role of cofactors in breakdown of TMAO in frozen red hake muscle, Journal Food Proc. Preserv. 7 (1983) 221.
[46] T. Mihori, H. Watanabe, An on-line method for predicting freezing time using time/temperature data collected in the early stages of freezing, Journal of Food Engineering 23 (1994) 357–373.
[47] A.C. Cleland, R.L. Earle, Freezing time predictions for foods—a simplified procedure, International Journal of Refrigeration 5 (1982) 134.
[48] A. de Michelis, A. Calvelo, Freezing time predictions for brick and cylindrical-shaped foods, Journal of Food Science 48 (1983) 909.
[49] Z. Saad, E.P. Scott, Analysis of accuracy in the numerical simulation of the freezing process in food materials, Journal of Food Engineering 31 (1997) 111.